Accurate Determination of the Complex Permittivity of Materials With Transmission Reflection Measurements in Partially Filled Rectangular Waveguides

José M. Catalá-Civera, Antoni J. Canós, Felipe L. Peñaranda-Foix, *Member, IEEE*, and Elias de los Reyes Davó

***Abstract*—An enhanced transmission reflection technique for the precise determination of the complex permittivity of dielectric materials partially filling the cross section of a rectangular waveguide is described. Dielectric properties are determined by an iterative procedure from two-port S-parameter measurements and a numerically generated propagation constant obtained from the analysis of a partially filled waveguide. Convergence of the solution is ensured from perturbational approximations. Unlike previous approaches, uncertainty investigation is performed, taking into account all the parameters involved in the dielectric characterization. Permittivity accuracy values are presented and, hence, an optimum measurement setup can be established. Measurements of reference materials have been carried out to validate the method.**

***Index Terms*—Accuracy study, dielectric properties, microwave measurements, rectangular waveguides.**

I. Introduction

THE precise permittivity determination of dielectric materials has been a very important task for ever-increasing microwave and millimeter-wave applications. Today, particularly with the extension of printed antennas, the electrical performance of a printed circuit board (PCB), for example, can be significantly affected by the dielectric properties of the substrate material [1]. Likewise, for the textile, polymer, and ceramic industries, the accurate knowledge of dielectric properties along with other parameters, such as moisture content, is essential for quality control and drying processes [2].

Several techniques for accomplishing these measurements have been described in the literature [3]. Transmission-line techniques based on one-port measurements [4]–[6] or two-port measurements [7]–[10] have been extensively used over the last 50 years. The Nicolson–Ross [7] and Weir (NRW) [8] procedures are the basis of these transmission/reflection (TR) techniques. In this method, the dielectric and magnetic properties of materials can be explicitly determined by measuring the scattering parameters of a coaxial or a waveguide cell loaded with a sample of dielectric, which completely fills the inner cross section. These formulas are, however, unstable at frequencies corresponding to sample lengths multiples of one half-wavelength for low-loss materials. An iterative procedure applicable to permittivity measurements is proposed in [9] to solve these instabilities. An analysis of the error sources of the measurements is also derived in [9], allowing to determine the effect of the sample configuration in the accuracy of the dielectric characterization. After a detailed analysis of NRW equations, an intermediate step is added in this procedure in [10], obtaining a noniterative method for dielectric materials. In all these waveguide TR techniques, only the fundamental mode propagation in the waveguide is supposed. The sample requirement of completely filling the guide's cross section is extremely difficult to be implemented for certain cases and, in practice, air gaps between the dielectric sample and conducting boundaries may exist [11], leading to the excitation of higher order modes. Thus, the validity bandwidth and permittivity range of the response may be shortened under this supposition.

Alternative techniques to these approaches reduce the width of the sample so that the guide is only partially filled, avoiding, in most cases, the air gaps effect. For instance, a dielectric material partially filling a slotted short-ended waveguide in the H-plane is used in [12] and [13]. The waveguide slab (WS) method reported in [14] involves inserting a dielectric substrate sample in a longitudinal slot in the center of the broad wall of a rectangular waveguide. Permittivity values are obtained from scattering measurements using approximations of the characteristic equations of the structure. The mode-matching method is used in [15] to analyze this discontinuity and extract the dielectric properties. In these methods, there is some ambiguity in the equations and a correct initial guess for the permittivity must be also provided.

Otherwise, in all these descriptions of partially filled waveguide techniques, systematic uncertainty studies have not been reported and, thus, the effect of the different sources of error in the accuracy of dielectric determination is unknown.

Hence, in this paper, we describe an iterative method for inferring the complex permittivity from a propagation constant extracted from experimental S-parameters, measured with a vectorial network analyzer (VNWA), and a numerically generated propagation constant in a partially filled waveguide. The inherent ambiguity in the transcendent equations is avoided with the aid of perturbational approximations so convergence of the correct solution is ensured. Unlike in previous approaches, an uncertainty analysis of the dielectric characterization is

Manuscript received February 7, 2001; revised October 19, 2001.

The authors are with the Departamento de Comunicaciones, Technical University of Valencia, 46071 Valencia, Spain (e-mail: jmcatala@dcom.upv.es).

Digital Object Identifier 10.1109/TMTT.2002.806940

0018-9480/03$17.00 © 2003 IEEE

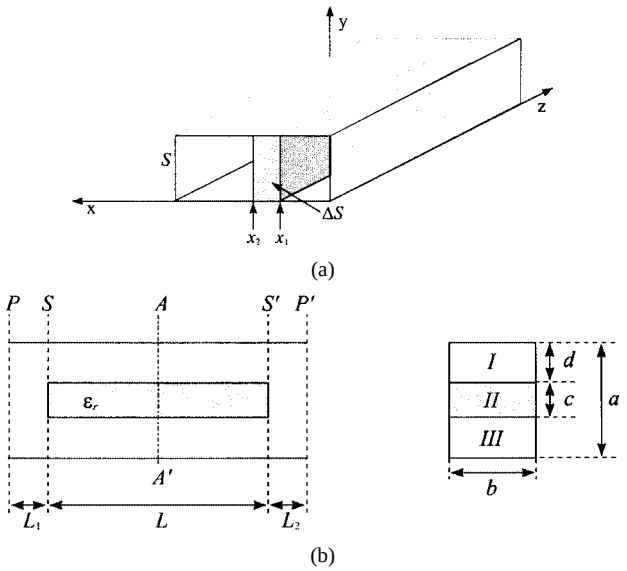

Fig. 1. Schematic of the partially filled structure. (a) Longitudinally loaded dielectric sample in the rectangular waveguide. (b) Geometry for the S-parameter measurement setup with material zone (II) and empty zones (I, III). Ports PP' denote calibration planes and SS' denote sample planes.

performed. Permittivity accuracy values are presented and, thus, optimum measurement setup can be established. By using this technique, a precise characterization of the complex permittivity is possible, thus overcoming some limitations of previous methods. In order to validate this procedure, some measurements of reference materials have been carried out and results have been compared to the literature.

II. Analytical Approach

A. Partially Filled Waveguides

Partially filled rectangular waveguides under analysis contain a dielectric material of relative permittivity $\varepsilon_r = \varepsilon_r' - j\varepsilon_r''$, with interfaces parallel to the E-field, as illustrated in Fig. 1.

This type of structures has been analyzed in the literature for several purposes [16]–[20]. In these waveguides, standard modes TE^z or TM^z cannot satisfy the boundary conditions of the structure, therefore, some other mode configurations may exist. These modes, transversals to the x-direction and referred as hybrid modes, are known as longitudinal section electric (LSE^x) modes, characterized by $E_x = 0$, and longitudinal section magnetic (LSM^x) modes, characterized by $H_x = 0$, and they can be obtained as combinations of the standard modes [21], [22]. The analysis of the problem is solved in this application with the aid of auxiliary vector potentials. For each region $\nu = I$, II, III (see Fig. 1), the fields are derived from auxiliary vector potentials $\vec{A}^{(\nu)}$ and $\vec{F}^{(\nu)}$ [22].

For LSE modes, electric and magnetic boundary conditions at the air–dielectric interfaces and some algebraic and trigonometric manipulations yield the characteristic equations of these modes as follows:

$$p \cdot \cot(pd) = q \cdot \mathrm{tg}\left(\frac{qc}{2}\right)$$
$$q \cdot \mathrm{tg}(pd) = -p \cdot \mathrm{tg}\left(\frac{qc}{2}\right). \quad (1)$$

The propagation constant $\gamma = \gamma^{(I)} = \gamma^{(II)} = \gamma^{(III)}$ in the waveguide relates the wavenumbers of each zone with the dielectric values of the material and, for nonmagnetic materials, it is given by

$$\gamma^2 = q^2 + \left(\frac{n\pi}{b}\right)^2 - \varepsilon_r k_0^2 = p^2 + \left(\frac{n\pi}{b}\right)^2 - k_0^2 \quad (2)$$

where ε_r is the relative complex permittivity of the dielectric region (II).

In a similar manner, for LSM modes, with some manipulations after applying the boundary conditions, the characteristic equations are derived similarly as follows:

$$q \cdot \cot(pd) = \varepsilon_r \cdot p \cdot \mathrm{tg}\left(\frac{qc}{2}\right)$$
$$q \cdot \cot(pd) = -\varepsilon_r \cdot p \cdot \cot\left(\frac{qc}{2}\right). \quad (3)$$

Equations (1) and (3) are multivalued transcendent equations of complex variable that determine the eigenvalues p and q. Each pair (p, q) with n value results in a different mode configuration in the waveguide. In (1) and (3), the first equations give odd modes and the second equations give even modes [21]. Total electric and magnetic fields in region $\nu (\nu = I, II, III)$ can be written as

$$\vec{E}^{(\nu)} = \sum_m \sum_n \vec{E}^{(\nu)}_{h,mn} + \vec{E}^{(\nu)}_{e,mn} \quad (4)$$
$$\vec{H}^{(\nu)} = \sum_m \sum_n \vec{H}^{(\nu)}_{h,mn} + \vec{H}^{(\nu)}_{e,mn} \quad (5)$$

where $\vec{E}^{(\nu)}_{h,mn}$, $\vec{H}^{(\nu)}_{h,mn}$, $\vec{E}^{(\nu)}_{e,mn}$, and $\vec{H}^{(\nu)}_{e,mn}$ represent LSE and LSM modal contribution to the total field, and they are derived from $\vec{A}^{(\nu)}$ and $\vec{F}^{(\nu)}$, respectively. Modal index m is related with the pair (p, q) by ordering the modes according to the cutoff frequencies determined as

$$f_c = \frac{c_0}{2\pi\sqrt{\varepsilon_r}}\sqrt{q^2 + \left(\frac{n\pi}{b}\right)^2} = \frac{c_0}{2\pi}\sqrt{p^2 + \left(\frac{n\pi}{b}\right)^2} \quad (6)$$

where c_0 denotes the light speed in vacuum. The first propagated mode or dominant mode is LSE_{10} ($m = 1$, $n = 0$), with characteristic impedance of guide

$$Z_1 = \frac{E_x}{H_y} = \frac{j\omega\mu_0}{\gamma} \quad (7)$$

being ω, the pulsation and μ_o, the vacuum permeability.

The discontinuity of the partially filled configuration of Fig. 1(a) directly excites LSE modes when the fundamental mode is incident because of the symmetries of the structure [18]. Therefore, the analysis can be reduced using the field expansion of only LSE modes. Frequency bandwidth is limited by the appearance of the first higher order mode LSE_{20}. In [21], this bandwidth is analyzed in function of the slab thickness. It is shown that, for relative width $c/a < 0.25$, the bandwidth in these waveguides is significantly increased. Furthermore, depending upon the permittivity of the material, there is a margin of relative width of the material where the bandwidth presents maximum values that can even double the bandwidth in complete filled waveguides. Therefore, the assumption of

only monomode propagation around these values can be considered and the localized effect of high-order modes neglected.

B. Perturbational Approximation

Equations (1)–(3) determine the relationship between dielectric parameters of the material and normalized eigenvalues in the waveguide. It is impossible to find an explicit relation between them because of their transcendent nature. However, perturbational techniques can provide approximate results under certain conditions of material thickness and dielectric properties.

Considering a waveguide of cross section S filled with air (ε_o) or dielectric (ε_r) and introducing a different dielectric sample of section ΔS (ε_r when air filled and ε_o when dielectric filled), as shown in Fig. 1(a), the change of the propagation constant of the waveguide caused by the introduction of this different material can be calculated as [23]

$$\gamma-\gamma_o=\frac{j\omega\int_{\Delta S}\left[(\varepsilon_r-\varepsilon_o)\vec{E}'^{*}_{o}\cdot\vec{E}'+(\mu_r-\mu_o)\vec{H}'^{*}_{o}\cdot\vec{H}'\right]\cdot ds}{\int_S\left(\vec{E}'^{*}_{o}\times\vec{H}'-\vec{H}'^{*}_{o}\times\vec{E}'\right)\cdot ds} \tag{8}$$

where subscript "o" signifies nonperturbed, while the rest corresponds to a perturbed waveguide. If the disturbance is assumed to have a small localized effect, with $\Delta S \ll S$ and electromagnetic fields $\vec{E}\cong\vec{E}_0$, $\vec{H}\cong\vec{H}_0$ outside the perturbing region, this expression can be broken up into algebraic equations where the dielectric constant and loss factor are related directly with the change in the phase constant (β) and attenuation factor (α), respectively. For the fundamental mode in the waveguide (TE_{10}), the perturbational formula is

$$\gamma-\gamma_o=\frac{\omega^2\mu_o}{2a\gamma_o}\,\varepsilon_o(\varepsilon_r-1)\left[\frac{\mathrm{sen}(K_c c)}{K_c}+(\phi-c)\right] \tag{9}$$

with

$$\phi=\begin{cases}0 & \text{air filled waveguide}\\ a & \text{dielectric filled waveguide}\end{cases}$$

where K_c is the cutoff wavenumber. Parameter ϕ indicates if the disturbance is due to the introduction of a dielectric slab (ε_r) in an empty waveguide, called *empty perturbational theory* or due to an air slab (ε_o) in a completely filled waveguide, called *full perturbational theory*. In particular, for a sample inserted in the waveguide assuming only fundamental mode propagation, phase constant (β) theoretically calculated from (1) and (2) and the perturbational approximations calculated from (9) are shown in Fig. 2 as a function of the relative width (c/a) and dielectric constant.

It is shown that, for thin sheets (low c/a), there is a good agreement between theoretical values and those given by the *empty perturbational approximation* (left-hand side). For large c/a relations, on the other hand, the agreement in the curves corresponds to the *full perturbational approximation* (right-hand side). It is interesting to see that, for some dielectric values (i.e., $\varepsilon'_r = 4$), the combination of both approximations (right- and left-hand side) and the real value are practically equal.

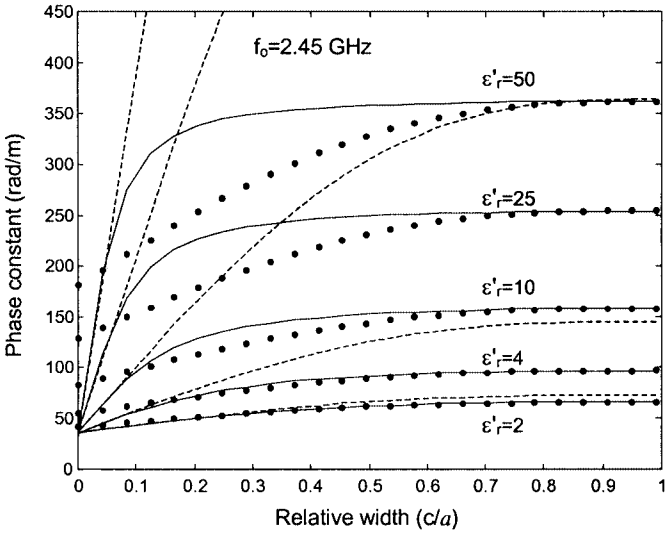

Fig. 2. Phase constant of the LSE_{10} mode obtained with the theoretical approach and perturbational approximations. Theoretical values are deonoted by the continuous line. Empty perturbational values are denoted by the dashed line and full perturbational theory is denoted by points. Sample height is b and loss factor is $\varepsilon''_r = 0.1$.

III. Description of the Method

The measurement procedure consists of placing a rectangular fragment of dielectric material inside the waveguide along the broad wall, as depicted in Fig. 1, and then measuring the S-parameters matrix of the structure with a VNWA. Calibration planes are P and P'. If the measured planes do not coincide with the sample plane, the response is shifted to planes S and S'.

The complex propagation constant of a partially filled waveguide of length L is extracted from the S-parameters, using the same formulation employed for those well-known completely filled waveguide techniques [8]–[10], assuming only fundamental-mode propagation. These equation are as follows:

$$K=\frac{S_{11}^2-S_{21}^2+1}{2\cdot S_{11}} \tag{10}$$

$$\Gamma=K\pm\sqrt{K^2-1} \tag{11}$$

$$T=\frac{S_{11}+S_{21}-\Gamma}{1-(S_{11}+S_{21})\cdot\Gamma} \tag{12}$$

$$T=e^{-\gamma L} \tag{13}$$

$$\Gamma=\frac{Z_1-Z_o}{Z_1+Z_o} \tag{14}$$

where S_{11} and S_{21} represent measured S-parameters versus frequency, Z_0 is the reference impedance, and Z_1 and γ are the impedance and propagation constant of the fundamental mode in the partially filled waveguide, respectively.

In order to finally determine the dielectric properties (ε_r), the aim is to solve numerically (1) and (2), which relates measured propagation constant (γ_{meas}) and complex permittivity. For this

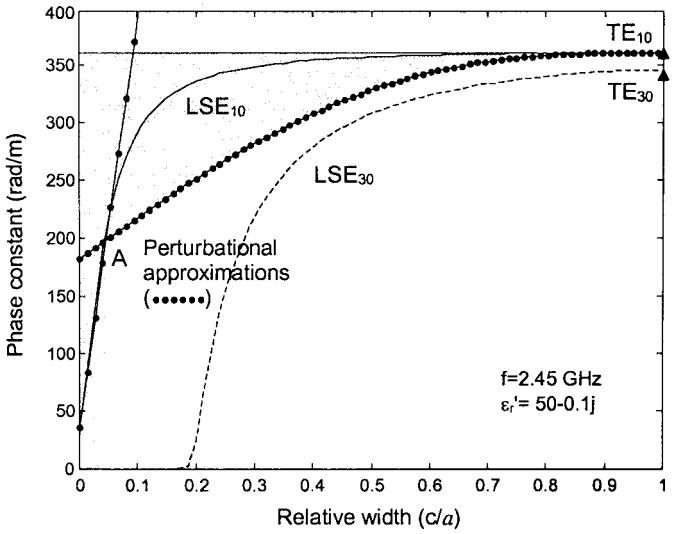

Fig. 3. First two solutions of the phase constant in a partially filled waveguide obtained with the theoretical approach and perturbational (empty and full) approximations. Theoretical values are denoted by the continuous line and perturbational values are denoted by points. The sample height is b.

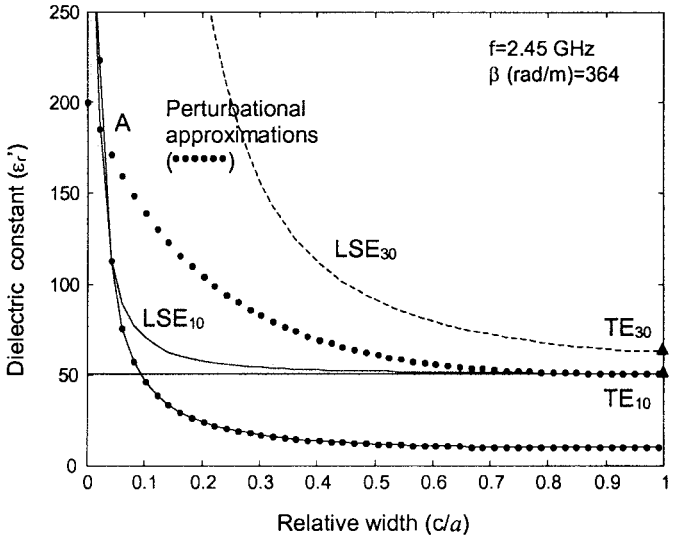

Fig. 4. Comparison of first two solutions of dielectric constant in a partially filled waveguide obtained with the theoretical approach (continuous line) and with perturbational approximations (points).

purpose, from (1) and (2), an error function f_e, defined as (15), is minimized as follows:

$$f_e(\varepsilon_r) = \frac{\cot\left(d\sqrt{\gamma_{\text{meas}}^2 + k_0^2}\right)}{\sqrt{\gamma_{\text{meas}}^2 + \varepsilon_r k_0^2}} - \frac{\text{tg}\left(\frac{c}{2}\sqrt{\gamma_{\text{meas}}^2 + \varepsilon_r k_0^2}\right)}{\sqrt{\gamma_{\text{meas}}^2 + k_0^2}}. \tag{15}$$

The minimization algorithm employed is based on a Newton–Raphson iterative routine that finds a bracketed root [24]. The algorithm uses in each step the relative complex permittivity as two variables, and the procedure is repeated until required convergence is obtained.

Since (15) presents multiple roots and we want to ensure a rapid convergence to the true solution, which is determined by the desired mode, this function is solved using an initial estimation and brackets selected from perturbational approximations and the strategy described in Section III-A. Once the dielectric properties have been determined for each frequency, these values are further used as the starting point for the following frequency.

Finally, the dielectric properties obtained with this technique are used to check (6) and to examine whether the obtained values can excite high order modes, which may invalidate the monomode assumption.

A. Convergence of Propagation Constant

Fig. 3 shows the first two solutions of phase constant in (1) corresponding to LSE_{10} and LSE_{30} modes, respectively, of a material of $\varepsilon_r = 50$ in function of the slab thickness. For instance, for $c/a = 0.5$, if the initial guess and brackets of the iteration procedure are not carefully selected, the solution provided by the minimization algorithm may not converge to the true solution.

However, if we represent the dielectric-filled waveguide solution (TE_{10}) and perturbational approximations (empty and full) of the first mode, the phase constant of the desired mode is now constrained by these values (shadowed area). Therefore, using these brackets in the numerical algorithm to solve (1), convergence to the true solution is ensured. Point A in Fig. 3 denotes the crossing of full and empty perturbation approximations. Thus, for c/a relations higher than point A, the inferior limit is fixed to the full perturbational response and initial guess to some midpoint into the shadowed area. For c/a relations lower than point A, the desired mode is delimited by the air- and dielectric-filled first mode (TE_{10}). An initial guess is given by the empty perturbational approximation. The same type of analysis was carried out with the attenuation factor (real part) in order to establish the limits of the minimization procedure. This strategy has shown its effectiveness until dielectric values around 95.

B. Convergence of Dielectric Properties

In a similar manner, Fig. 4 shows the first two solutions of dielectric constant calculated from (15) of a waveguide of phase constant $\beta = 364$ in function of the slab thickness. As above, if brackets are not properly selected, the solution provided by the iterative algorithm may not converge to the true solution.

As can be seen, perturbational approximations again delimit the desired solution into the shadowed area. Thus, following a similar procedure such as that in Fig. 3, for c/a values lower than point A (crossing point between empty and full perturbational approximations), the upper limit in the iteration procedure is fixed to the full perturbational approximation given by (9) and the lower extremum given by the dielectric-filled waveguide solution. For c/a relations lower than point A, brackets are dielectric and air-filled waveguide solutions. The same type of analysis can be applied to the imaginary part of the permittivity (loss factor).

IV. Accuracy of the Method

The accuracy in the permittivity determination depends upon the influence of the different sources of error on the measurements. These sources of error include material homogeneity,

TABLE I
ERROR PARAMETERS (A, B) OF (17) IN FUNCTION OF THE SOURCE OF ERROR $|\chi_i|$

$\lvert\chi_i\rvert\rightarrow$	$\lvert S_{11}\rvert$	θ_{11}	$\lvert S_{21}\rvert$	θ_{21}
A	$\frac{S_{11}}{\lvert S_{11}\rvert}$	jS_{11}	$\frac{S_{11}}{\lvert S_{11}\rvert}$	jS_{11}
B	$\frac{-1+S_{11}^2+S_{21}^2}{2S_{11}\lvert S_{11}\rvert}$	$\frac{j\left(-1+S_{11}^2+S_{21}^2\right)}{2S_{11}}$	$\frac{-S_{21}^2}{S_{11}\lvert S_{11}\rvert}$	$-j\frac{S_{21}^2}{S_{11}}$

unascertained sample and waveguide dimensions, waveguide losses, high-order modes excitation, and the systematic uncertainty of the instrumentation used to perform the S-parameter measurements. Waveguide losses and length can be determined and the effect subtracted from the sample measurements. The nonexistence of high-order modes is checked out using (6), leaving the core of the error to the sample position, unascertained sample dimensions, and mainly to the precision of the network analyzer. This measurement uncertainty analysis can be accomplished using the partial derivative technique of (1), (2), and (13), following the same procedures as some previously reported TR techniques [9], [10]. The solved equation is reproduced in (16), shown at the bottom of this page.

In (16), we can see that the uncertainty is separately evaluated, where $\Delta|S_{11}|$, $\Delta|S_{21}|$ represents the uncertainty of the modulus and $\Delta|\theta_{11}|$, $\Delta|\theta_{21}|$ represents the uncertainty of the phase of the S_{11}- and S_{21}-parameters, respectively, which directly depend on the VNWA and calibration procedure specifications [25]. ΔL is the uncertainty in the sample length. Operating with the derivatives in (16), the following formulas are obtained:

$$\frac{\partial\varepsilon_r}{\partial|\chi_i|}=\frac{2\gamma}{K_o^2}\,\frac{q-pf_1}{pf_1}\left(\frac{-e^{\gamma L}}{L}\right)\cdot\frac{A(1-\Gamma^2)+B\left(1\pm\dfrac{PK}{\sqrt{K^2-1}}\right)\left((S_{11}+S_{21})^2-1\right)}{\left[1-\Gamma(S_{11}+S_{21})\right]^2} \tag{17}$$

where

$$f_1=\frac{\operatorname{tg}\left(\dfrac{qc}{2}\right)+\dfrac{qc}{2}\sec^2\left(\dfrac{qc}{2}\right)}{\cot(pd)-pd\cdot\csc^2(pd)} \tag{18}$$

and the parameters A and B depend upon the source of error ($|\chi_i|$), as illustrated in Table I.

For the unascertained sample length, the equation is

$$\frac{\partial\varepsilon_r}{\partial|L|}=\frac{2\gamma}{K_o^2}\,\frac{pf_1-q}{pf_1}\left(\frac{\gamma}{L}\right). \tag{19}$$

In Figs. 5 and 6, this total uncertainty is represented for the material's dielectric constant and loss factor, respectively, as a function of the normalized sample length (L/λ_g) for various values of permittivity at a $c/a=0.25$ relative width. The plotted error has made use of the precision of the VNWA, with full two-port calibration procedure specifications [25].

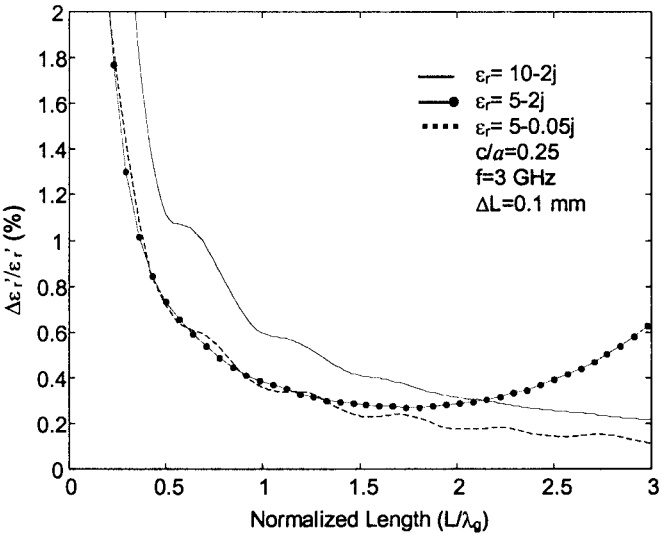

Fig. 5. Relative total uncertainty of dielectric constant (ε_r') as a function of normalized length (L/λ_g) for several values of permittivity.

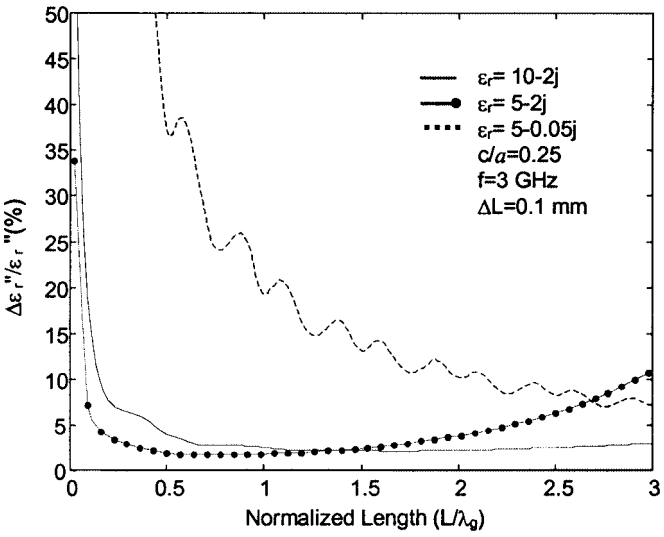

Fig. 6. Relative total uncertainty of loss factor (ε_r'') as a function of normalized length (L/λ_g) for several values of permittivity.

The results show that the uncertainties continue to decrease as a function of increasing length. Based on the results from these figures, a longer sample is preferred to improve the accuracy. We can also see in Fig. 6 that the total relative error for low-loss materials is very large, which confirms the low performance of TR measurements for this kind of materials. For this case, alternative techniques, such as resonant methods, are recommended.

$$\Delta\varepsilon_r=\sqrt{\left(\frac{\partial\varepsilon_r}{\partial|S_{11}|}\,\Delta|S_{11}|\right)^2+\left(\frac{\partial\varepsilon_r}{\partial\theta_{11}}\,\Delta\theta_{11}\right)^2+\left(\frac{\partial\varepsilon_r}{\partial|S_{21}|}\,\Delta|S_{21}|\right)^2+\left(\frac{\partial\varepsilon_r}{\partial\theta_{21}}\,\Delta\theta_{21}\right)^2+\left(\frac{\partial\varepsilon_r}{\partial L}\,\Delta L\right)^2} \tag{16}$$

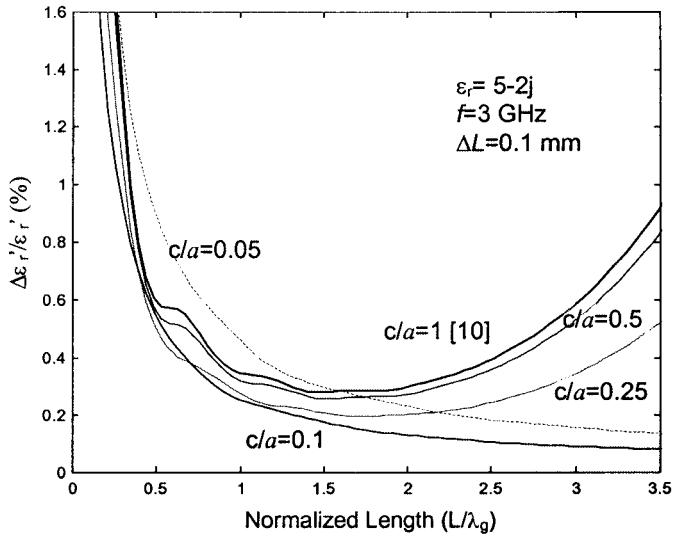

Fig. 7. Comparison of relative total uncertainty of dielectric constant obtained with TR measurements in complete-filled waveguides [10] with that determined using the procedure in partially filled structures as a function of normalized length for several values of slab thickness.

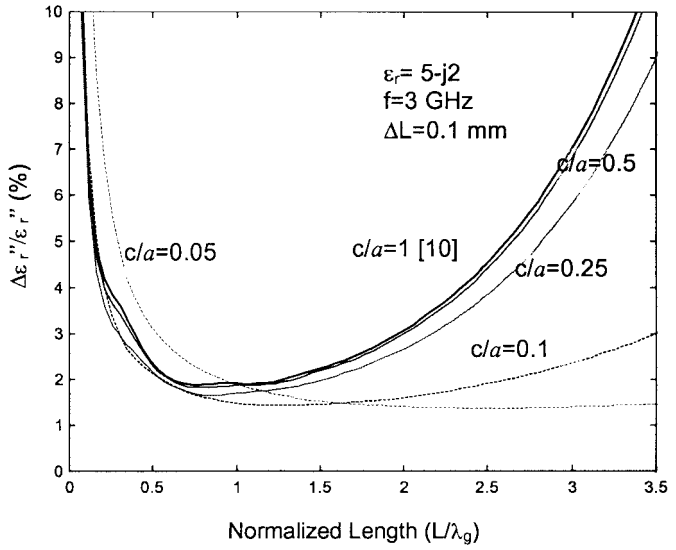

Fig. 8. Comparison of relative total uncertainty of loss factor obtained with TR measurements in complete-filled waveguides [10] with that determined using the procedure in partially filled structures, as a function of normalized length for several slab thicknesses.

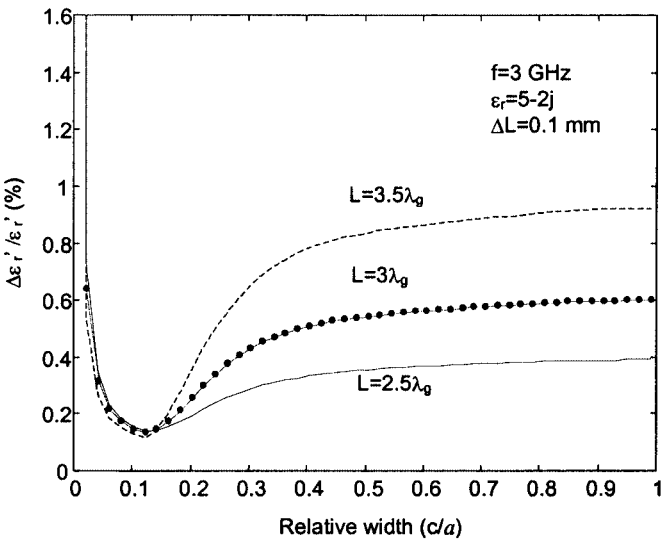

Fig. 9. Relative total uncertainty of dielectric constant (ε_r') as a function of relative width of the material in the waveguide for several values of sample length.

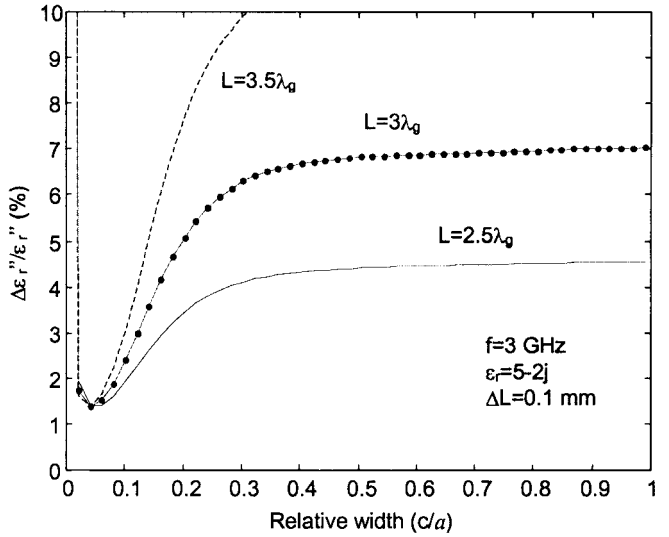

Fig. 10. Relative total uncertainty of loss factor (ε_r'') as a function of relative width of the material in the waveguide for several values of sample length.

Figs. 7 and 8 show the effect of reducing the width of the material inserted in the waveguide on the accuracy. In these simulations, we have chosen the same reference materials used by Baker-Jarvis *et al.* in [9] and Bougriet *et al.* in [10] to compare accuracy in partially filled structures with those calculated with completely filled waveguides. For this purpose, the error calculated in (16) has been reproduced considering a waveguide cell instead of a coaxial line, as reported in [10], and the results are also plotted in Figs. 7 and 8. Sample length is normalized here with the dielectric-filled wavelength to better compare the curves.

In accordance to other TR methods, the total uncertainty usually tends to decrease as a function of the increasing sample length and then it begins to increase again. This is mainly attributable to large values of $\Delta|S_{21}|$ for low transmitted signals in longer samples. When reducing the width of the material, we can observe in both figures that this error is delayed to higher frequencies from the complete waveguide case, and this delay is much higher with narrower samples. This effect may be associated to the reduction of the total material volume in the waveguide for the same sample length, which increments the transmitted signal (S_{21}) avoiding values of $\Delta|S_{21}|$ being as large as in complete-filled waveguides. This reduction presents, however, a limit with excessively narrow samples, where the error increments again (i.e., $c/a = 0.05$) due to large values of $\Delta|S_{11}|$. This improvement in the accuracy is better shown in Figs. 9 and 10, where the relative uncertainty in the measurements is represented as a function of the relative width of the material in the waveguide for a given value of sample length.

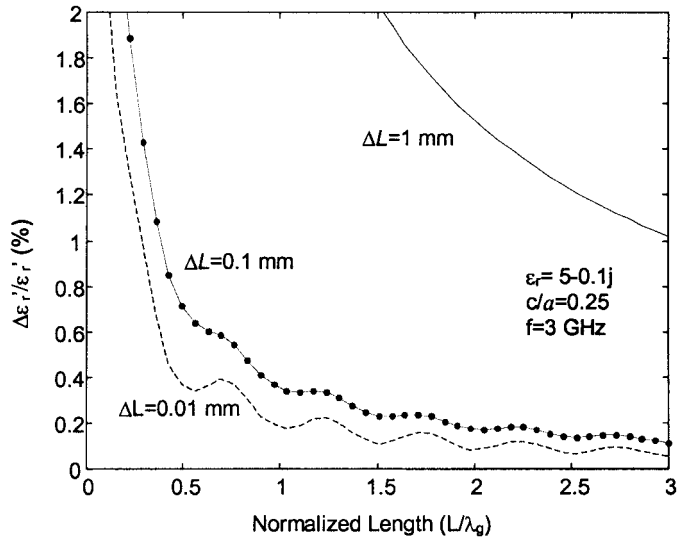

Fig. 11. Relative total uncertainty of dielectric constant (ε_r') as a function of normalized length for several values of unascertained sample dimensions.

As depicted, the uncertainty in the samples that completely fill the waveguide ($c/a = 1$) is continuously reduced with the use of narrower samples ($c/a < 1$), except for excessive narrow samples, where again, this value is increased. Furthermore, for all sample length plotted in this figure, there is a width (c/a) for which the error presents a minimum (around $c/a = 0.1$). For the loss factor in the material, as illustrated in Fig. 10, the uncertainty error can be improved from 10% to 1.5%, which is quite significant. As previously mentioned, these reductions are only appreciated for high or moderate losses; meanwhile for low-loss materials, no minimum peaks are observed.

The effect of another important source of error, the unascertained sample dimensions, which, in turn, yields to uncertainties in the location of the reference planes of the scattering parameters, is plotted in Fig. 11.

From this figure, it is clearly observed that small uncertainties in the sample dimensions and, particularly in the positioning of the sample in the waveguide, can introduce important errors in the dielectric characterization.

V. Measurements and Results

The approach described above was used to measure the complex permittivity of PVC and a dielectric substrate, typically used for printed antenna design. Dielectric properties of these materials are well documented and can be used to validate the behavior of the method. The HP-8720B Network Analyzer was used to measure the scattering matrix over the frequency in a WR-340 waveguide holder. Suitable sample lengths were chosen from preliminary measurements. Results are given in Figs. 12 and 13.

Fig. 12 shows the complex permittivity of PVC in function of the frequency obtained using a 20-mm-thick sample of material placed at the center of the waveguide. From this figure, we can see the good agreement of the complex permittivity of PVC obtained using this method, with the value used as in [26]. The accuracy of the dielectric determination was lower than 0.25% and 6% for real and imaginary parts, respectively.

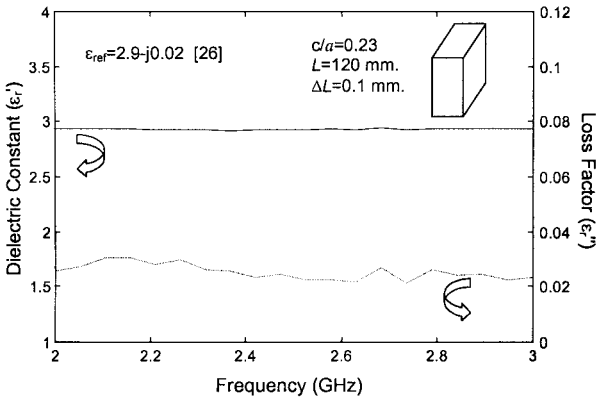

Fig. 12. Complex permittivity of a PVC sample as a function of frequency obtained using the procedure in partially filled waveguides. Reference value from [26].

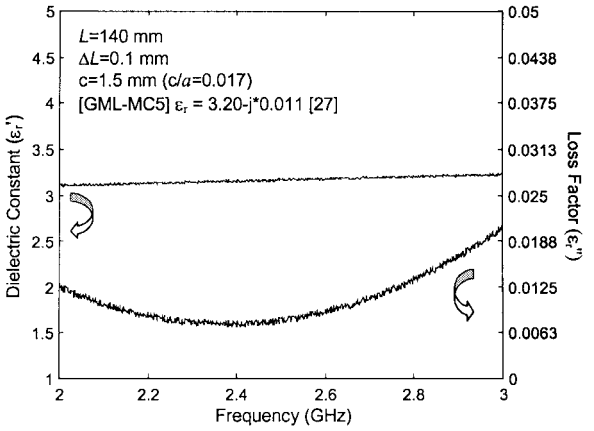

Fig. 13. Complex permittivity of an unclad dielectric substrate of moderate losses as a function of frequency obtained using the procedure in partially filled waveguides. Reference value from [27].

Fig. 13 shows the complex permittivity of a 1.5-mm-thick dielectric substrate (GML-MC5), measured in the rectangular waveguide, between 2–3 GHz. To place the substrate in the waveguide, a longitudinal centered nonradiating slot was drilled in the upper and lower sides of the waveguide. Also, additional metal shields around the edges of the sample in the slot can be used to suppress undesirable radiation. An appropriate sample length was also chosen from preliminary measurements. The calculated values present good agreement with the complex permittivity value provided by the manufacturer, and this is also plotted in Fig. 13 as a reference value [27]. The accuracy of the dielectric determination, for an uncertainty of 0.1 mm in the sample length, results in errors lower than 1% in the dielectric constant. However, for this relative width, the loss factor error reaches up to 50%. Both values are in concordance with those previously presented in the accuracy study for very thin samples.

VI. Conclusions

An enhanced technique based on TR measurements for the determination of the complex permittivity of materials partially filling the cross section of a rectangular waveguide has been described. The method is based on the analysis of partially filled

rectangular waveguides, which leads to transcendent equations that are numerically solved by providing a bracketed initial estimation from perturbational approximations, thus ensuring the convergence of the solution. Uncertainty analysis has been performed and measurement setup can be optimized in order to improve the accuracy of results. The study allows us to conclude that the permittivity accuracy obtained by using partially filled waveguides is higher than that obtained in completely filled structures, besides overcoming the air-gaps problem. Uncertainty is particularly decreased with relative sample widths around 0.1. It is also followed from the investigation that special care must be taken with very thin materials since uncertainty reaches very high values.

ACKNOWLEDGMENT

The authors wish to particularly acknowledge GIL Technologies, Southampton, U.K., for providing the unclad dielectric substrates measured in this paper.

REFERENCES

[1] G. T. Lei, R. W. Techentin, and B. K. Gilbert, "Electrical behavior of multichip modules in the presence of power and ground plane noise," in *IEEE Proc. Int. Multichip Modules Conf.*, Denver, CO, Apr. 1995, pp. 175–184.

[2] J. Monzo-Cabrera, J. M. Catala-Civera, and E. de los Reyes, "Study of kinetics of combined microwave and hot air drying of leather," *J. Soc. Leather Technologists and Chemists*, vol. 84, no. 1, pp. 38–43, Feb. 2000.

[3] J. Baker-Jarvis, R. G. Geyer, J. H. Grosvenor, Jr., M. D. Janezic, C. A. Jones, B. Riddle, C. M. Weil, and J. Krupka, "Dielectric characterization of low-loss materials, A comparison of techniques," *IEEE Trans. Dielect. Elect. Insulation*, vol. 5, pp. 571–577, Aug. 1998.

[4] S. Roberts and A. R. Von Hippel, "A new method for measuring dielectric constant and loss in the range of centimeter waves," *J. Appl. Phys.*, vol. 17, pp. 610–616, 1946.

[5] M. C. Decréton and M. S. Ramachandraiah, "Nondestructive measurement of complex permittivity for dielectric slabs," *IEEE Trans. Microwave Theory Tech.*, vol. MTT-23, pp. 1077–1080, Dec. 1975.

[6] K. Sarabandi and F. T. Ulaby, "Technique for measuring the dielectric constant of thin materials," *IEEE Trans. Instrum. Meas.*, vol. 37, pp. 631–636, Dec. 1988.

[7] A. M. Nicolson and G. F. Ross, "Measurement of the intrinsic properties of materials by time domain techniques," *IEEE Trans. Instrum. Meas.*, vol. IM-19, pp. 377–382, Nov. 1970.

[8] W. B. Weir, "Automatic measurement of complex dielectric constant and permeability at microwave frequencies," *Proc. IEEE*, vol. 62, pp. 33–36, Jan. 1974.

[9] J. Baker-Jarvis, E. Vanzura, and W. Kissick, "Improved technique for determining complex permittivity with the transmission reflection method," *IEEE Trans. Microwave Theory Tech.*, vol. 38, pp. 1096–1103, Aug. 1990.

[10] A. H. Boughriet, C. Legrand, and A. Chapton, "Noniterative stable transmission/reflection method for low-loss material complex permittivity determination," *IEEE Trans. Microwave Theory Tech.*, vol. 45, pp. 52–57, Jan. 1997.

[11] K. S. Champlin and G. H. Glover, "'Gap effect' in measurement of large permittivities," *IEEE Trans. Microwave Theory Tech.*, vol. MTT-14, pp. 397–398, Aug. 1966.

[12] I. J. Bahl and H. M. Gupta, "Microwave measurement of dielectric constants of liquids and solids using partially laded slotted waveguide," *IEEE Trans. Microwave Theory Tech.*, vol. MTT-22, pp. 52–54, Jan. 1974.

[13] P. I. Somlo, "A convenient self-checking method for the automated microwave measurement of μ and ε," *IEEE Trans. Instrum. Meas.*, vol. 42, pp. 213–216, Apr. 1993.

[14] R. A. York and R. C. Compton, "An automated method for dielectric constant measurements of microwave substrates," *Microwave J.*, vol. 33, pp. 115–122, Mar. 1990.

[15] C. Jiang and C. Yang, "Complex permittivity and permeability measurement for high-loss material in a waveguide," *Microwave Opt. Technol. Lett.*, vol. 9, no. 1, pp. 41–43, May 1995.

[16] N. Eberhardt, "The field displacement filter—A new family of disipative waveguide filters," in *IEEE MTT-S Int. Microwave Symp. Dig.*, 1966, pp. 90–93.

[17] F. Arndt, D. Grauerholz, and R. Vahldieck, "Theory and design of low-insertion loss fin-line filters," *IEEE Trans. Microwave Theory Tech.*, vol. MTT-30, pp. 155–163, Feb. 1982.

[18] F. Arndt, J. Bornemann, and R. Vahldieck, "Design of multisection impedance-matched dielectric-slab filled waveguide phase shifters," *IEEE Trans. Microwave Theory Tech.*, vol. MTT-32, pp. 34–39, Jan. 1984.

[19] N. Eberhardt, "Propagation in the off center E-plane dielectrically loaded waveguide," *IEEE Trans. Microwave Theory Tech.*, vol. MTT-15, pp. 282–289, May 1967.

[20] F. E. Gardiol, "Higher-order modes in dielectrically loaded rectangular waveguides," *IEEE Trans. Microwave Theory Tech.*, vol. MTT-16, pp. 919–924, Nov. 1968.

[21] P. H. Vartanian, W. P. Ayres, and A. L. Helgesson, "Propagation in dielectric slab loaded rectangular waveguide," *IRE Trans. Microwave Theory Tech.*, vol. MTT-5, pp. 215–222, Apr. 1958.

[22] C. A. Balanis, *Advanced Engineering Electromagnetics*. New York: Wiley, 1989, pp. 394–410.

[23] J. L. Altman, *Microwave Circuits*. New York: Van Nostrand, 1964, pp. 409–416.

[24] W. H. Press, S. A. Teukolsky, W. T. Vetterling, and B. P. Flannery, *Numerical Recipes in C. The Art of Scientific Computing*, 2nd ed. Cambridge, U.K.: Cambridge Univ. Press, 1992, pp. 347–393.

[25] "Materials measurement: Measuring the dielectric constant of solids with the HP 8510 network analyzer," Hewlett-Packard, Santa Rosa, CA, Product Note 8510-3, 1985.

[26] C. Wan, B. Nauwelaers, W. De Raedt, and M. Van Rossum, "Two new measurement methods for explicit determination of complex permittivity," *IEEE Trans. Microwave Theory Tech.*, vol. 46, pp. 1614–1619, Nov. 1998.

[27] *GIL Technologies Product Catalog*, GIL Technol., Southampton, U.K., 1998.

Jose M. Catalá-Civera was born in Valencia, Spain, on February 15, 1969. He received the Dipl.Ing. and Ph.D. degrees in telecommunications engineering from the Universidad Politécnica de Valencia, Valencia, Spain, in 1993 and 2000, respectively.

From 1993 to 1996, he was a Research Assistant with the Microwave Laboratory, Universidad Politécnica de Valencia, where he developed several prototypes for industrial applications of microwave engineering. Since 1996, he has been with the Departamento de Comunicaciones, Universidad Politécnica de Valencia, where he is currently an Associate Professor responsible for the Microwave Laboratory. His research interests encompass all aspects related to microwave theory and applications, the use of microwaves for dielectric heating, microwave filters, microwave resonators, measurement of dielectric properties, and development of microwave sensors for nondestructive testing of materials.

Antoni J. Canós was born in Almenara (Castelló de la Plana), Spain, on March 17, 1973. He received the Dipl.Ing. degree in telecommunications engineering from the Universitat Politècnica de València, Valencia, Spain, in 1999, and is currently working toward the Ph.D. degree in microwave nondestructive testing of materials and monitoring of processes at the Universitat Politècnica de València.

From 1999 to 2001, he was a Research Assistant with the Microwave Heating Group (G.C.M.). In 2001, he joined the Departament de Comunicacions, Universitat Politècnica de València, as an Associate Lecturer and he joined the Institute for the Applications and Advanced Communication Technologies (ITACA), Valencia, Spain, as a Research and Development Engineer. His current research interests include numerical analysis and design of waveguide components, measurement techniques and devices for the electromagnetic characterization of materials, and noninvasive monitoring of processes involving dielectric changes.

Felipe L. Peñaranda-Foix (S'93–M'00) was born in Benicarló, Spain, in 1967. He received the M.S. degree in electrical engineering from the Universidad Politécnica de Madrid, Madrid, Spain, in 1992, and the Ph.D. degree in electrical engineering from the Universidad Politécnica de Valencia, Valencia, Spain, in 2001.

In 1992, he joined the Departamento de Comunicaciones, Universidad Politécnica de Valencia, where he is currently a Senior Lecturer. His current research interests includes electromagnetic scattering, microwave circuits, and microwave heating applications.

Elias de los Reyes Davó was born in Albatera, Spain, on February 6, 1950. He received the Dipl.Ing. degree from the Universidad Politécnica de Madrid, Madrid, Spain, in 1974, and the Ph.D. degree in telecommunications engineering from the Universidad Politécnica de Barcelona, Barcelona, Spain, in 1978.

In 1986, he achieved a tenured position as a Professor of radar technology with the Universidad Politécnica de Barcelona. In 1988, he joined the Universidad Politécnica de Valencia, Valencia, Spain, where he has been Vice-Dean of the Telecommunication School, Dean of the Communications Department, and Vice-Chancellor of research. He is currently the Dean of the Telecommunications School and Acting Director of the Institute for the Applications and Advanced Communication Technologies (ITACA), where he is the leader of the Applied Electromagnetic Group (GEA). He has authored or coauthored over 100 technical papers and three technical books. His research interests are high-power microwave systems and their industrial applications.

Dr. de los Reyes Davó was chairman of the 7th International Conference on Microwave Heating in 1999.